Modeling of enhanced field confinement and scattering by optical wire antennas

Andrea Locatelli[1*], Costantino De Angelis[1], Daniele Modotto[1], Stefano Boscolo[2], Francesco Sacchetto[2], Michele Midrio[2], Antonio-D. Capobianco[3], Filippo M. Pigozzo[3], and Carlo G. Someda[3]

[1]*Consorzio Nazionale Interuniversitario per le Scienze Fisiche della Materia (CNISM), Dipartimento di Elettronica per l'Automazione, Università degli Studi di Brescia, via Branze 38, Brescia 25123, Italy.*

[2]*Dipartimento di Ingegneria Elettrica, Gestionale e Meccanica, Università degli Studi di Udine, via delle Scienze 208, Udine 33100, Italy.*

[3]*Dipartimento di Ingegneria dell'Informazione, Università degli Studi di Padova, via Gradenigo 6/b, Padova 35131, Italy.*

[*]*andrea.locatelli@ing.unibs.it*

Abstract: We describe the application of full-wave and semi-analytical numerical tools for the modeling of optical wire antennas, with the aim of providing novel guidelines for analysis and design. The concept of antenna impedance at optical frequencies is reviewed by means of finite-element simulations, whereas a surface-impedance integral equation is derived in order to perform an accurate and efficient calculation of the current distribution, and thereby to determine the equivalent-circuit parameters. These are introduced into simple circuits models, directly borrowed from radio frequency, which are applied in order to model the phenomena of enhanced field confinement at the feed gap and light scattering by optical antennas illuminated by plane waves.

OCIS codes: (130.3120) Integrated optics devices; (350.4238) Nanophotonics; (050.6624) Subwavelength structures; (260.3910) Metal optics; (240.6680) Surface plasmons.

References and links

1. S. A. Maier, *Plasmonics: Fundamentals and Applications* (Springer, 2007).
2. E. Ozbay, "Plasmonics: merging photonics and electronics at nanoscale dimensions," Science **311,** 189–193 (2006).
3. J. J. Greffet, "Nanoantennas for light emission," Science **308,** 1561 (2005).
4. L. Novotny, "Optical antennas tuned to pitch," Nature (London) **455,** 887 (2008).
5. P. Mühlschlegel, H. J. Eisler, O. J. F. Martin, B. Hecht, and D. W. Pohl, "Resonant optical antennas," Science **308,** 1607–1608 (2005).
6. T. H. Taminiau, F. D. Stefani, F. B. Segerink, and N. F. van Hulst, "Optical antennas direct single-molecule emission," Nature Photon. **2,** 234–237 (2008).
7. P. Ghenuche, S. Cherukulappurath, T. H. Taminiau, N. F. van Hulst, and R. Quidant, "Spectroscopic mode mapping of resonant plasmon nanoantennas," Phys. Rev. Lett. **101,** 116805–(1–4) (2008).
8. R. L. Olmon, P. M. Krenza, A. C. Jones, G. D. Boreman, and M. B. Raschke, "Near-field imaging of optical antenna modes in the mid infrared," Opt. Express **16,** 20295–20305 (2008).
9. M. Schnell, A. García-Etxarri, A. J. Huber, K. Crozier, J. Aizpurua, and R. Hillenbrand, "Controlling the near-field oscillations of loaded plasmonic nanoantennas," Nature Photon. **3,** 287–291 (2009).
10. L. Novotny, "Effective wavelength scaling for optical antennas," Phys. Rev. Lett. **98,** 266802–(1–4) (2007).
11. A. Alù, and N. Engheta, "Input impedance, nanocircuit loading, and radiation tuning of optical nanoantennas," Phys. Rev. Lett. **101,** 043901–(1–4) (2008).

#113740 - $15.00 USD Received 7 Jul 2009; revised 30 Jul 2009; accepted 31 Jul 2009; published 4 Sep 2009

12. A. Alù, and N. Engheta, "Tuning the scattering response of optical nanoantennas with nanocircuit loads," Nature Photon. **2,** 307–310 (2008).
13. R. W. P. King, "The linear antenna - eighty years of progress," Proceedings of the IEEE **55,** 2–16 (1967).
14. C. A. Balanis, *Antenna theory: analysis and design* (Wiley, 2005).
15. S. J. Orfanidis, *Electromagnetic waves and antennas*, http://www.ece.rutgers.edu/∼orfanidi/ewa/, (2008).
16. R. Kappeler, D. Erni, C. Xudong, and L. Novotny, "Field computations of optical antennas," Journ. of Computational and Theoretical Nanoscience **4,** 686–691 (2007).
17. H. Fischer, and O. J. F. Martin, "Engineering the optical response of plasmonic nanoantennas," Opt. Express **16,** 9144–9154 (2008).
18. J. Aizpurua, G. W. Bryant, L. J. Richter, F. J. Garcia de Abajo, B. K. Kelley, and T. Mallouk, "Optical properties of coupled metallic nanorods for field-enhanced spectroscopy," Phys. Rev. B **71,** 235420–(1–13) (2005).
19. G. W. Hanson, "On the applicability of the surface impedance integral equation for optical and near infrared copper dipole antennas," IEEE Trans. Antennas Propag. **54,** 3677–3685 (2006).
20. G. W. Hanson, "Radiation efficiency of nano-radius dipole antennas in the microwave and far-infrared regimes," IEEE Antennas Propag. Magazine **50,** 66–77 (2008).
21. R. W. P. King, and T. T. Wu, "The imperfectly conducting cylindrical transmitting antenna," IEEE Trans. Antennas Propag. **14,** 524–534 (1966).
22. J. A. Stratton, *Electromagnetic theory* (McGraw-Hill, 1941).
23. J. Wen, S. Romanov, and U. Peschel, "Excitation of plasmonic gap waveguides by nanoantennas," Opt. Express **17,** 5925–5932 (2009).
24. J. S. Huang, T. Feichtner, P. Biagioni, and B. Hecht, "Impedance matching and emission properties of nanoantennas in an optical nanocircuit," Nano Lett. **9,** 1897–1902 (2009).
25. COMSOL Multiphysics 3.5, COMSOL Inc. (http://www.comsol.com).
26. CST Microwave Studio 2009, Darmstadt, Germany.
27. R. E. Collin, "Limitations of the Thévenin and Norton equivalent circuits for a receiving antenna," IEEE Antennas Propag. Magazine **45,** 119–124 (2003).

1. Introduction

The continuous technological advancement in electronic and optical materials at the nanoscale is quickly leading to the design of devices which were not even conceivable a few years ago. Among the areas that are gaining most from these advancements, we may certainly quote plasmonics [1, 2], and optical antennas [3, 4]. In fact, recent years have witnessed an impressive amount of experimental [5–9] and theoretical work [10–12] on optical devices conceived to efficiently couple free-space propagating light with localized excitation of either light emitters or receivers, for a wide variety of potential applications, including on-chip communication, ultra-dense data storage, efficient solar cells, near-field optical microscopy and spectroscopy.

Clearly, antennas have been in common use at radio frequencies (RF) for more than a century. Well-assessed design rules have been developed in time, and are now available, at RF, for different antenna families. This is true in particular for the oldest type of antenna: the linear wire aerial [13–15]. Our goal here is to find an efficient way to determine a good approximation of the current distribution in a center-fed wire antenna at optical frequencies. This will enable us to evaluate its near and far field, and thereafter to extrapolate theoretically the antenna equivalent-circuit parameters which, up to now, have been evaluated only through full-wave numerical simulations, which are inevitably marked by heavy computational burdens [11, 12, 16–18]. Moreover, we will demonstrate that simple circuit models directly borrowed from RF permit to quantitatively predict both the field enhancement at the feed gap and the power scattered by the optical antenna when it is illuminated by a plane wave.

At first sight, these tasks may look simple, given that, as well known, Maxwell's equations are scale invariant (provided the scale contraction factor is the same for all lengths, including wavelength, and the electromagnetic properties of the materials do not depend on frequency). In fact, there are at least two reasons why the tasks are not simple at all. One is related to the available fabrication technology, the second is related to the optical properties of available bulk materials.

As far as nanotechnologies are concerned, making very thin metal rods is still an open issue

#113740 - $15.00 USD Received 7 Jul 2009; revised 30 Jul 2009; accepted 31 Jul 2009; published 4 Sep 2009

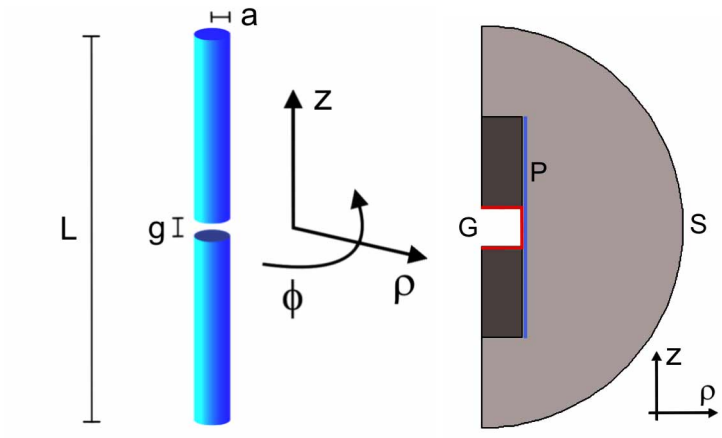

(a) (b)

Fig. 1. Schematic view of a cylindrical dipole antenna (not in scale) fed at its center. (a) 3D view with reference frame; notice that the origin is in the middle of the gap region. *L*: length of the dipole; *g*: gap thickness; *a*: radius of the rod. (b) View of the 2D computational domain used for the full-wave simulations: the red line (*G*) indicates the delta-gap surface, the blue line (*P*) denotes the region with the probe for the azimuthal component of the magnetic field, *S* is the semi-spherical boundary (radius 300 nm).

[7, 8]. As a consequence, as opposed to what is common and normal at RF, in the optical domain we will always be considering thick wires, and going to lose the simplifying initial assumptions known as the thin wire approximation [13–15]. As far as materials are concerned, what makes a big difference between RF and optics is that at RF we can usually assume to deal with perfect electric conductors; this assumption does not hold for optical antennas. As a matter of fact, the process of building design rules for optical antennas has to start from scratch, by following essentially the same way that was chosen in 1897 for radio frequency: first, the current distribution on an imperfectly conducting and thick (i.e., radius of the cylindrical rod not very small compared to rod length and to the wavelength) cylindrical antenna must be evaluated by exploiting an integral equation approach, and then simple equivalent circuits are used in order to study the antenna behavior.

2. Integral equation model

In this Section we briefly recall the formulation of the integral equation (the so-called Pocklington's equation [14, 15]) that will be used in order to determine the approximated current distribution in optical wire antennas, in analogy with what has been done in Refs. [19, 20]. Every antenna, no matter whether receiving or transmitting, can be thought of as driven by a "primary" external field $\vec{E}_{in}(x,y,z)$, due either to the generator connected to the antenna terminals (in the transmitting mode), or to the impinging wave (in the receiving mode). This incident field $\vec{E}_{in}(x,y,z)$ induces a current I in the wire, and the current in turn generates a radiated electric field $\vec{E}(x,y,z)$. It is possible to solve the electromagnetic problem by specifying the boundary conditions for the total field $\vec{E}_{tot}(x,y,z) = \vec{E}(x,y,z) + \vec{E}_{in}(x,y,z)$ on the antenna surface. For wire antennas parallel to the z axis (see Fig. 1(a)), neglecting the role played by the two flat circular surfaces at the ends of the cylinder, these boundary conditions read [21]:

$$E_{z,tot}(z, \rho = a) = I(z) Z_s \, , \, |z| \leq \frac{L}{2} \, . \tag{1}$$

#113740 - $15.00 USD Received 7 Jul 2009; revised 30 Jul 2009; accepted 31 Jul 2009; published 4 Sep 2009

It follows that:

$$E_z(z,\rho=a) = I(z)Z_s - E_{z,in}(z,\rho=a)\,. \tag{2}$$

The surface impedance per unit length Z_s for a cylindrical rod can be defined as [22]

$$Z_s = \frac{\gamma J_0(\gamma a)}{2\pi a\sigma J_1(\gamma a)}\,, \tag{3}$$

where

$$\gamma = (1-j)\sqrt{\frac{\omega\mu_0\sigma}{2}}\,, \tag{4}$$

and σ is the conductivity of metal. Assuming purely a surface current at $\rho = a$, we have:

$$\vec{J} = \vec{J}_s(z)\delta(\rho-a) = \hat{z}I(z)\delta(\rho-a)\frac{1}{2\pi a}\,, \tag{5}$$

hence the z-component of the magnetic vector potential reads [14]:

$$\begin{aligned} A_z(z,\rho) &= \frac{\mu}{4\pi}\int_{-L/2}^{L/2} I(z')K(z-z',\rho)dz'\,,\\ K(z-z',\rho) &= \frac{1}{2\pi}\int_0^{2\pi}\frac{\exp(-ik_0R)}{R}d\phi'\,, \end{aligned} \tag{6}$$

and

$$R = \sqrt{(x-x')^2+(y-y')^2+(z-z')^2} = \sqrt{(z-z')^2+\rho^2+a^2-2\rho a\cos(\phi')}\,, \tag{7}$$

where (x,y,z) is the observation point, and (x',y',z') are the coordinates of the line-source $I(z)$ located on the wire surface at $\rho = a$ [14]. Once we know A_z, we can compute the electric field generated by the current $I(z)$:

$$(\partial_z^2 + k_0^2)A_z = i\omega\mu\varepsilon E_z\,. \tag{8}$$

Introducing Eq. (2) into Eq. (8) we then get:

$$(\partial_z^2+k_0^2)\frac{\mu}{4\pi}\int_{-L/2}^{L/2} I(z')K(z-z',\rho=a)dz' = i\omega\mu\varepsilon\left(I(z)Z_s - E_{z,in}(z,\rho=a)\right)\,, \tag{9}$$

i.e. Pocklington's equation for optical wire antennas [19, 20]. Eq. (9) has been solved through the Moment Method (MoM) to find $I(z)$; the excitation has been modeled by using a 1-V delta-gap source [14, 15], thus $E_{z,in}(z,\rho=a)$ was fixed to a constant value $1/g$ over the whole feed gap region, and was zero elsewhere. The input impedance has been evaluated as the ratio between the imposed voltage and the current in the middle of the wire $I_0 = I(z=0)$.

3. Antenna impedance modeling

An accurate characterization of the antenna input impedance is a key issue also at optical frequencies, in particular (but not only) for the design of nanocircuits consisting of receiving and emitting nanoantennas connected by plasmonic waveguides. Indeed, it has recently been demonstrated that coupling between different plasmonic elements can be studied by using impedance matching techniques which are well established at RF [23, 24].

We took as reference example a cylindrical dipole antenna made of silver (described by a Drude model with $\varepsilon_\infty = 5$, plasma frequency $f_p = 2.175$ PHz and collision frequency $\gamma = 4.35$

#113740 - $15.00 USD Received 7 Jul 2009; revised 30 Jul 2009; accepted 31 Jul 2009; published 4 Sep 2009

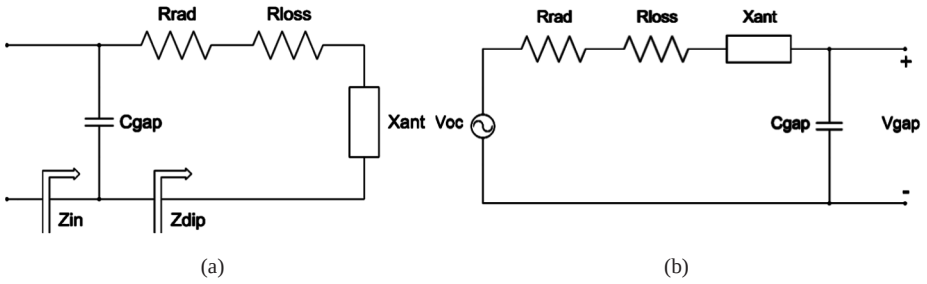

Fig. 2. a) Antenna impedance Z_{in} seen at the gap terminals. b) Thévenin equivalent circuit in the receiving mode. R_{rad}: radiation resistance; R_{loss}: loss resistance; X_{ant}: antenna reactance; C_{gap}: gap capacitance; V_{oc}: open-circuit voltage.

THz) and immersed in air, with length $L = 110$ nm, radius of the metal rods $a = 5$ nm and gap thickness $g = 3$ nm [11, 12]. Finite-element simulations [25] were performed in order to calculate the input impedance of the antenna. We exploited the intrinsic axial symmetry of the problem to reduce the computational domain to two dimensions (see Fig 1(b)). The structure was excited through a delta-gap source [14, 15], by imposing a value of the z-component of the electric field E_z on the boundary G (see the red line) so that the voltage across the gap is unity. The azimuthal component of the magnetic field H_ϕ on the antenna surface has been recorded (the probe region is depicted by the blue line P) and it allowed to get the total current flowing into the cylinder, calculated as circulation of the magnetic field. The input impedance was defined as the ratio between the imposed voltage and the current in the middle of the gap I_0. Fig. 2(a) shows the circuit model that we have used to represent the optical antenna in the transmitting mode [14]. It is worth saying that the gap region was outside of the computational domain (see Fig. 1(b)), therefore the full-wave simulations supplied the intrinsic dipole impedance Z_{dip}; the input impedance Z_{in} seen at the terminals was then obtained through the parallel combination between Z_{dip} and the reactance due to the gap capacitance [11, 12]. Note that we will use throughout the paper the notation which is more popular among electrical engineers ($Z_{in,dip} = R_{in,dip} + jX_{in,dip}$).

In Fig. 3 we report the calculated antenna impedance between 200 and 700 THz (i.e. about 430 and 1500 nm, from the visible to the near-infrared). The results coming from finite-element simulations and the solution of Pocklington's equation exhibit excellent agreement over the entire bandwidth, in fact both in the case of the real (Fig. 3(a)) and the imaginary part of Z_{in} (Fig. 3(c)) the curve which represents the FEM solution of Maxwell's equations (solid red line) and the one with data from the semi-analytical model (dashed black line) are overlapped. Good agreement emerges also after comparison with the results reported in [11, 12], which have been obtained by using a commercial software tailored for RF modeling [26]. In contrast with our case, the authors performed the excitation by using predefined input ports, thus the calculation supplied the input impedance Z_{in}, whereas Z_{dip} was obtained by de-embedding the gap reactance.

Further FEM simulations were performed in order to verify the accuracy of the antenna impedance modeling. In particular, we calculated the radiated power P_{rad} flowing out of the external surface S, and then we determined the radiation resistance as $R_{rad} = 2P_{rad}/|I_0|^2$; moreover, we evaluated the ohmic losses P_{loss} into the metal and then the loss resistance $R_{loss} = 2P_{loss}/|I_0|^2$. Both R_{rad} and R_{loss} are depicted in Fig. 3(b), and the radiation efficiency $\eta = R_{rad}/(R_{rad} + R_{loss})$ has been evaluated: η is about 28% at the first open-circuit resonance and decreases rapidly to zero with increasing frequency, again in good qualitative agreement

#113740 - $15.00 USD Received 7 Jul 2009; revised 30 Jul 2009; accepted 31 Jul 2009; published 4 Sep 2009

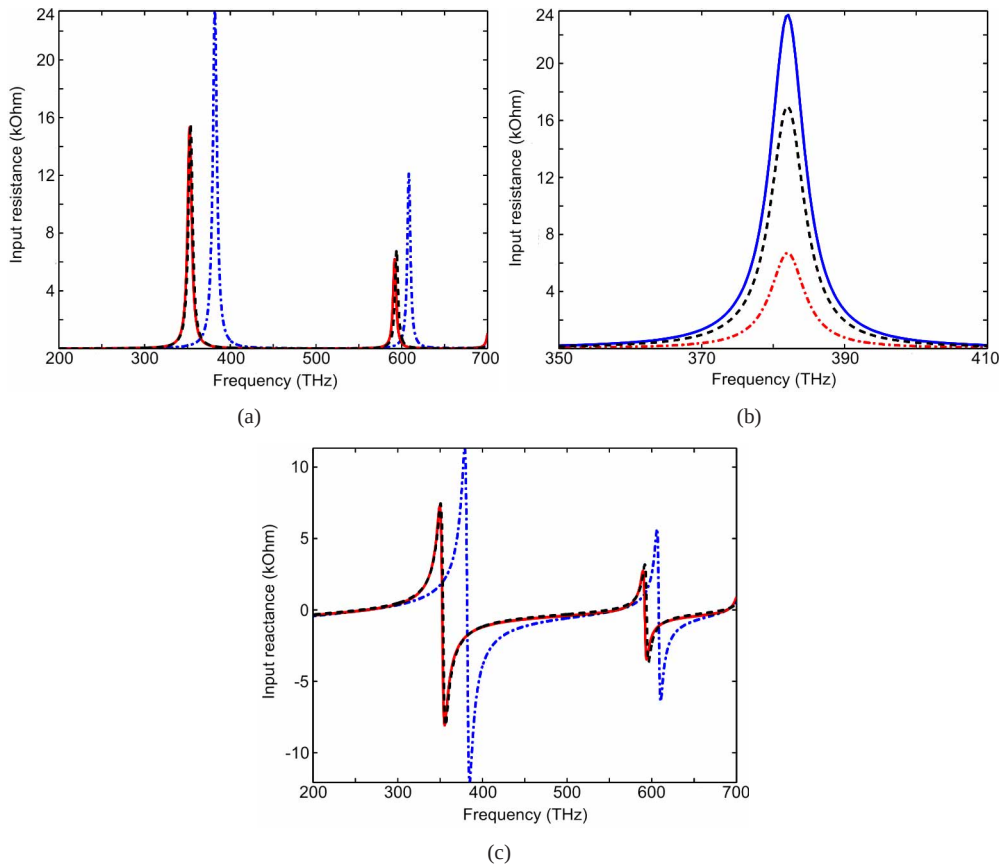

Fig. 3. a) R_{dip} calculated from FEM simulations (dashed-dotted blue line); R_{in} evaluated from the parallel combination of Z_{dip} and the gap reactance (solid red line), and from Pocklington's equation (dashed black line). b) R_{rad} (dashed-dotted red line), R_{loss} (dashed black line), and $R_{rad}+R_{loss}$ (solid blue line, overlapped with the R_{dip} curve) obtained from FEM simulations. c) X_{dip} calculated from FEM simulations (dashed-dotted blue line); X_{in} evaluated from the parallel combination of Z_{dip} and the gap reactance (solid red line), and from Pocklington's equation (dashed black line).

with [11]. As a final validation of our treatment it is important to emphasize that the resistance calculated as ratio between the voltage imposed by the delta-gap source and the total current flowing into the feed gap is equal to the sum of the radiation and loss resistances R_{rad} and R_{loss} (see Fig. 3(b), the two curves are overlapped).

4. Field enhancement and light scattering modeling

The possibility of achieving strong field enhancement on a nanometer scale in the antenna feed gap is certainly one of the main reasons that triggered research in the area of optical antennas in the last years [3–9]. Here we will demonstrate that the integral equation model described in Section 2 can be used in order to predict quantitatively field enhancement by optical antennas, without resorting to full-wave simulations; moreover, we will show that the analysis of a simple circuit model can provide a better physical insight into the optical antenna operation.

Let us consider the circuit model for the antenna in the receiving mode depicted in Fig. 2(b).

#113740 - $15.00 USD Received 7 Jul 2009; revised 30 Jul 2009; accepted 31 Jul 2009; published 4 Sep 2009

V_{oc} is the open-circuit voltage due to the incident field, and the voltage V_{gap} at the terminals of the gap capacitance is just what we need in order to calculate the electric field into the gap, in fact $|E_z(0,0,0)| = |V_{gap}|/g$. We investigated three different routes to the evaluation of the field enhancement at the feed gap. The most straightforward way to reach the goal is to perform finite-element simulations with a plane wave (with amplitude $E_0 = 1$ V/m) impinging on the antenna, by recording the value of the electric field in the middle of the feed gap (Fig. 4(a), solid red line). It is worth noting that in the receiving mode the computational domain was modified with respect to Fig. 1(b) by adding the gap region. As an alternative method, the current distribution $I(z)$ calculated through finite-element simulations in the transmitting mode has been used, by exploiting the reciprocity theorem, to evaluate the antenna effective length through the well-known formula [15]:

$$L_{eff} = \frac{1}{I_0}\int_{-L/2}^{L/2} I(z')dz', \tag{10}$$

and the open-circuit voltage has been determined as $V_{oc} = E_0 L_{eff}$ (Fig. 4(a), dashed-dotted blue line). The voltage V_{gap} has been calculated by writing the simple equation of the voltage divider $V_{gap} = V_{oc} \cdot Z_c/(Z_c + Z_{dip})$ (Fig. 4(a), dotted green line), where Z_c is the impedance associated with the presence of the gap and $Z_{dip} = R_{dip} + jX_{ant}$. Last, but not least, $I(z)$ obtained as solution of Pocklington's equation permits to calculate the field enhancement in a very efficient and accurate way. In this case Eq. (10) and the following one give directly V_{gap} (Fig. 4(a), dashed black line), since the effect of the gap reactance is already included in the calculation, as it is clear from the previously reported simulations of the input impedance (see Fig. 3). It is worth noting the excellent agreement between the values of V_{gap} obtained from the three different methods, therefore we can conclude that the semi-analytical model based on Pocklington's equation and the simple circuit model can be useful tools for analysis and design of devices conceived for field localization beyond the diffraction limit.

We have also investigated the application of the circuit model in Fig. 2(b) for the evaluation of the power scattered by the antenna when it is illuminated by a plane wave. It is worth saying that, in this case, we resorted to full-wave simulations also for the calculation of the circuit model parameters, since knowledge of the radiation resistance R_{rad} was necessary (see Section 3). Finite-element simulations were performed in order to get a reference solution of the electromagnetic problem, by calculating the scattered power flowing out of a closed surface surrounding the antenna (Fig. 4(b), solid red line). The results obtained from the calculation of the power dissipated by R_{rad} within the Thévenin equivalent circuit show that the circuit model perfectly captures amplitude and position of the peak corresponding to the open-circuit resonance, but a non-physical peak appears near the maximum value of R_{dip} at 381 THz (Fig. 4(b), dashed-dotted black line). We repeated the same calculation by using the Norton equivalent circuit, and also in that case the real peak is accurately reproduced, whereas a spurious peak near the first null of X_{dip} (around 264 THz) is present (Fig. 4(b), dashed blue line). Notice that the Thévenin and Norton circuits are equivalent only at their terminals. Limitations of these circuit models for the analysis of receiving antennas have been clearly illustrated in the literature [27]. In particular, in our case the Norton and Thévenin circuits supply the real scattered power summed up with the power scattered by the short- (peak at 264 THz) and open-circuited antenna (peak at 381 THz) respectively [27]. We can conclude that circuit modeling can be used to study also scattering by optical wire antennas, but results from the Thévenin and Norton equivalent circuits must be carefully interpreted by taking into account the presence of spurious peaks.

From the designer's point of view, the simulations we have reported highlight that there is a strong relationship between input impedance, field enhancement and light scattering by the

#113740 - $15.00 USD Received 7 Jul 2009; revised 30 Jul 2009; accepted 31 Jul 2009; published 4 Sep 2009

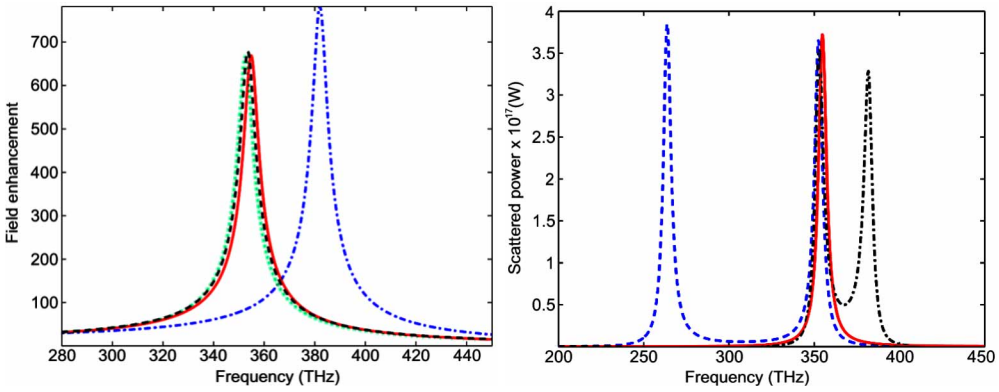

(a) (b)

Fig. 4. a) Open-circuit voltage $|V_{oc}|$ (divided by the gap thickness g) calculated from FEM simulations (dashed-dotted blue line); field enhancement evaluated from the circuit model in Fig. 2(b) (dotted green line), from Pocklington's equation (dashed black line), and from FEM simulations with plane-wave excitation (solid red line). b) Scattered power calculated from FEM simulations with plane-wave excitation (solid red line), from the circuit model in Fig 2(b) (dashed-dotted black line), and from the Norton equivalent circuit (dashed blue line).

antenna. In particular, it is worth noting that both field enhancement and scattered power reach the maximum value when the real part of Z_{in} (R_{in}) is maximum (around 355 THz). According to the circuit model, that frequency corresponds to the first open-circuit resonance, i.e. when the antenna and gap reactance have equal magnitude and opposite sign. This means that the concept of antenna loading at optical frequencies [12] could be applied also to tune the frequency of maximum field enhancement, or viceversa this huge sensitivity to the optical properties of the gap region could be used for sensing applications.

In this work we have focused the attention on a specific optical wire antenna taken as reference example, but we have applied all the reported techniques to many antennas characterized by different geometrical parameters. In particular, we focused our attention on the set of devices analyzed in [11], and all the results exhibit the same behavior we have described above. We also varied the gap thickness and the radius of the cylindrical rod, and solution of Pocklington's equation provided good results even when we narrowed the feed gap region or we reduced the wire aspect ratio (length over diameter) to values around 5.

5. Conclusion

We have described the application of numerical tools, combined with simple circuit models, for analysis and design of optical wire antennas. The definition of input impedance at optical frequencies has been thoroughly reviewed by means of finite-element simulations, and an integral equation model based on Pocklington's equation has been used in order to predict in an efficient and accurate way both input resistance and reactance. The phenomena of enhanced field confinement at the feed gap and light scattering by optical antennas have been studied, and an excellent agreement between different modeling techniques has been demonstrated. We believe that the reported treatment is only one of the first steps toward the application, in the field of optics, of techniques which are more popular in the context of circuit theory and radio frequency, with the aim of giving simple guidelines for the development of optical nanocircuits.

#113740 - $15.00 USD Received 7 Jul 2009; revised 30 Jul 2009; accepted 31 Jul 2009; published 4 Sep 2009

Acknowledgment

The authors acknowledge financial support from Ministero dell'Istruzione, dell'Università, e della Ricerca in the framework of the PRIN 2007 programme, and from University of Padova, project CPDA081514/08.

#113740 - $15.00 USD Received 7 Jul 2009; revised 30 Jul 2009; accepted 31 Jul 2009; published 4 Sep 2009